

Published in final edited form as:

Traffic. 2012 December ; 13(12): 1653–1666. doi:10.1111/tra.12009.

A common clathrin-mediated machinery coordinates cell-cell adhesion and bacterial internalization

Matteo Bonazzi^{1,2,3,7,*}, Andreas Kühbacher^{1,2,3}, Alejandro Toledo-Arana⁴, Adeline Mallet⁵, Lavanya Vasudevan⁶, Javier Pizarro-Cerdá^{1,2,3}, Frances M. Brodsky⁶, and Pascale Cossart^{1,2,3,*}

¹Institut Pasteur, Unité des Interactions Bactéries-Cellules, Paris, F-75015 France

²Inserm, U604, Paris, F-75015 France

³INRA, USC2020, Paris, F-75015 France

⁴Laboratory of Microbial Biofilms, Instituto de Agrobiotecnología, Universidad Pública de Navarra-CSIC-Gobierno de Navarra, Campus de Arrosadía, 31006 - Pamplona, Spain

⁵Institut Pasteur, Plateforme de Microscopie Ultrastructurale, Imagopole, Paris, France

⁶The G.W. Hooper Foundation, Departments of Bioengineering and Therapeutic Sciences, of Microbiology and Immunology and of Pharmaceutical Chemistry, University of California, San Francisco, San Francisco, CA 94143-0552, USA

Abstract

Invasive bacterial pathogens often target cellular proteins involved in adhesion as a first event during infection. For example, *Listeria monocytogenes* uses the bacterial protein InlA to interact with E-cadherin, hijack the host adherens junction machinery, and invade non-phagocytic cells by a clathrin-dependent mechanism. Here we investigate a potential role for clathrin in cell-cell adhesion. We observed that the initial steps of adherens junction formation trigger the phosphorylation of clathrin, and its transient localization at forming cell-cell contacts. Furthermore, we show that clathrin serves as a hub for the recruitment of proteins that are necessary for the actin rearrangements that accompany the maturation of adherens junctions. Using an InlA/E-cadherin chimera, we show that adherent cells expressing the chimera form adherens junctions with cells expressing E-cadherin. To model bacterial invasion, we demonstrate that non-adherent cells expressing the InlA chimera can be internalized by E-cadherin-expressing adherent cells. Together these results reveal that a common clathrin-mediated machinery may regulate internalization and cell adhesion and that the relative mobility of one of the interacting partners plays an important role in the commitment to either one of these processes.

Introduction

Cell-cell adhesion is a fundamental process in organogenesis and development. It is subject to finely tuned regulation that determines the transition from a mesenchymal to an epithelial state. Adult cells that escape this regulation become prone to metastatic development, and loss of cell adhesion is one of the main determinants of cancer [1]. Eukaryotic proteins involved in cell adhesion are often the targets of pathogens that adhere to and invade host cells [2-4]. Recently, our laboratory reported a fundamental role for clathrin in the actin-dependent internalization of *Listeria monocytogenes*, a bacterium that invades the host cell

*To whom correspondence should be addressed, matteo.bonazzi@cpbs.cnrs.fr, pcossart@pasteur.fr.

⁷Present address: CNRS, UMR 5236, CPBS, F34965, Montpellier, France

using the surface protein internalin (InIA) to interact with the cell adhesion molecule E-cadherin [5-7]. This suggested the possibility of a link between clathrin, actin and cell adhesion. E-cadherin is the cell surface protein responsible for establishment of adherens junctions (AJ) [8,9], which form as a result of homotypic calcium-dependent interactions between E-cadherins on neighbouring cells. Initial interaction produces so-called immature junctions. Then, E-cadherin clustering and downstream signalling are required for junction maturation and reorganization of the underlying actin cytoskeleton from branches to cables [10-12].

During InIA-mediated infection, *Listeria* activates the non-receptor tyrosine kinase Src, which initiates a series of post-translational modifications to proteins that are key to bacterial internalization, including cortactin and E-cadherin [5,13]. Bacterial internalization also involves the clathrin-dependent endocytosis machinery [7] in a newly described synergy with actin polymerization that is distinct from conventional clathrin-mediated endocytosis. We recently established that during *Listeria* infection, clathrin recruitment is accompanied by tyrosine phosphorylation of the clathrin heavy chain (CHC), an event that occurs prior to and is required for actin recruitment to bacterial entry sites [7,14]. CHC is the subunit of clathrin that mediates self-assembly of the clathrin coat and its tyrosine phosphorylation by Src-family kinases is a feature of sustained clathrin presence at sites of signaling receptors [15-17]. The associated clathrin light chain (CLC) subunit mediates clathrin-actin interactions via binding of Hip1R [18-24]. Interestingly, transcellular E-cadherin/E-cadherin interactions at the onset of AJ formation also activate Src [25,26]. Furthermore, we observed previously that both InIA- and E-cadherin-coated latex beads are internalized by a clathrin-mediated pathway [5]. Together, these observations led us to investigate whether the clathrin/actin interactions characteristic of bacterial invasion may also be involved in E-cadherin-mediated cell-cell adhesion. Here we show that the onset of E-cadherin-mediated cell-cell adhesion triggers clathrin recruitment and CHC phosphorylation. In addition, clathrin recruitment is required for F-actin rearrangements during AJ maturation, which we show also depends on CLC and Hip1R. Finally, we expressed an InIA/E-cadherin chimeric protein at the surface of HeLa cells, to recapitulate, using epithelial cells, the host-pathogen interactions that result in the internalization of *L. monocytogenes*. By doing so, we show that a common clathrin-mediated machinery controls cell-cell adhesion or engulfment of non-adherent cells, the latter mimicking bacterial internalization.

Results

CHC is recruited at cell-cell contacts and is required for adherens junction formation

Interaction of the *Listeria* surface protein InIA with its host receptor E-cadherin triggers a) tyrosine phosphorylation of CHC b) clathrin accumulation at the plasma membrane and c) clathrin-dependent actin rearrangement at bacterial entry sites [14]. We addressed whether these events are also triggered by E-cadherin/E-cadherin interactions during the formation of adherens junctions. We first analyzed the distribution of phosphorylated CHC (pCHC) in freshly seeded JEG3 cells that established new AJs using an antibody specific for pCHC [14]. Cells were subjected to cytosolic extraction before antibody labeling, to improve the detection of pCHC at the plasma membrane. 16 hours after seeding, pCHC showed extensive colocalization with E-cadherin and actin at sites of cell-cell contacts, in contrast with the distribution of total CHC detected with mAb X22 [27], which displayed typical perinuclear enrichment of clathrin in the trans-Golgi network region, as well as plasma membrane staining (Fig. 1a). This suggests that, similar to bacterial infections, E-cadherin/E-cadherin interactions can trigger the phosphorylation and stabilization of CHC at the plasma membrane. We then followed the dynamics of clathrin recruitment to cell-cell contacts by applying the calcium jump assay to MDCK cells transfected with GFP-tagged

CLC. AJs were first allowed to dissociate by incubating cells in calcium-free medium. Upon re-addition of calcium we observed the recruitment of clathrin to cell-cell contacts over a period of 15h (Fig. 1b and Movie S1). Cells were then fixed and labeled for E-cadherin and actin. Clathrin was recruited at cell-cell contacts in 70% of cells 12h after re-addition of calcium, which represented a marked increase as compared to the 40% of cells at steady state (not subjected to the calcium jump; Fig. 1c). To address the role of clathrin at cell-cell contacts during AJ formation, Jeg3 cells were depleted of CHC by RNA interference and allowed to form new cell-cell contacts. As expected, CHC-depleted cells lost the pCHC recruitment at cell-cell contacts (Fig. 1a), though internal staining was less sensitive to siRNA depletion, as previously observed [43]. Notably however, we observed that in these cells, the strong localization of actin at cell-cell junctions was severely disrupted (Fig. 1a). Indeed, control-treated cells exhibited a sharp and narrow (20 pixels in average) peak of actin fluorescence at cell-cell contacts, that corresponded to an equal peak of E-cadherin (Fig. 2a, charts 1 and 2). In CHC-depleted cells E-cadherin still accumulated at AJs (Fig. 2c), although in many cases the fluorescence was spread out and covered an average of 40 pixels (Fig. 2b, charts 3 and 4). More importantly, accumulation of E-cadherin did not correspond to that of actin, which remained diffused or weakly concentrated at cell-cell junctions (Fig. 2b, charts 3 and 4, Fig. 2c).

Ultrastructural analysis by Correlative Light Scanning Electron Microscopy (CLSEM) showed that cells treated with control siRNA displayed thick (50 nm) actin cables parallel to cell-cell contacts (Fig. 3a SEM insets) that co-localized with the phalloidin signal detected by light microscopy (Fig. 3a SEM + actin). In CHC-depleted cells however, actin was organized in branched structures that are more typical of migrating cells, with scarce, very thin actin cables at cell-cell contacts (Fig. 3b SEM insets).

Finally, to discriminate between a defect in actin polymerization at the AJ and a change in actin organization, we compared the localization of the Arp2/3 complex (by using an anti p34 antibody) and mDia at cell-cell contacts between control cells and cells depleted of CHC, after cytosolic extraction. In control cells, both proteins showed a diffused cytoplasmic localization with an enrichment at sites of cell-cell contacts where they co-localized with E-cadherin and actin (Fig. S1b and c). Interestingly, despite the alteration of actin morphology observed at cell-cell contacts following CHC depletion, the localization of either p34 or mDia was only mildly affected by the same treatment (Fig. S1b and c). Together, our data indicate that, during the formation of AJs, phosphorylated clathrin is recruited at cell-cell contacts where it plays a role in recruitment and organization of the actin cytoskeleton, similar to what we have previously observed during bacterial infections.

The clathrin-actin interaction machinery is recruited at forming cell-cell contacts

Our recent observations suggest that, during infection, clathrin serves as a platform for the recruitment of a set of proteins that link F-actin to clathrin at bacteria/cell adhesion sites [14]. These include the clathrin adaptor Dab2, the actin-binding protein Hip1R and the motor protein Myosin VI. To test the possibility that clathrin plays a similar role during the formation of AJs, we followed the recruitment of Hip1R, Myosin VI and Dab2 at cell-cell contacts in Jeg3 cells that established new AJs. In all cases, these proteins colocalized with E-cadherin and actin at sites of cell-cell contacts (Fig. 4a). After incubation of Jeg3 cells beyond 24 h, allowing the maturation of AJs, the detected amount of these proteins at cell-cell contacts decreased (data not shown). We next investigated a potential role for the clathrin-actin interaction machinery during the formation of AJs by depleting Jeg3 cells of the above-mentioned proteins, including clathrin light chain (CLC), and allowed cells to form new AJs. The depletion of CLC, Dab2, and, to a minor extent, that of Myosin VI, considerably reduced the presence of actin at cell-cell junctions, similarly to what we had previously observed when CHC was depleted (Fig. S2). The depletion of Hip1R resulted in

a milder phenotype, which is potentially attributed to the partial efficiency of the siRNA treatment (Fig. S2).

To address whether clathrin and associated components of the clathrin/actin machinery could directly influence AJ formation downstream of E-cadherin/E-cadherin complex formation or whether their depletion indirectly affects other aspects of AJ formation, we recapitulated AJ formation using the minimal system of E-cadherin-coated beads. These beads adhere to and eventually are internalized by E-cadherin-expressing cells [5]. First, Jeg3 cells were incubated with E-cadherin-coated beads for 1 h and the recruitment of Dab2, Myosin VI and Hip1R was followed by fluorescence microscopy. All three proteins were recruited, together with actin, at the bead entry sites (Fig. 4b). We then individually depleted Dab2, Myosin VI and Hip1R from Jeg3 cells, using 2 independent siRNA sequences for each, and tested treated cells for bead internalization. The depletion of each protein efficiently reduced the recruitment of actin around beads and the subsequent internalization of E-cadherin-coated beads (Fig. 4c). These bead studies indicate that formation of the clathrin-actin platform is directly downstream of formation of E-cadherin/E-cadherin complexes and that its disruption inhibits actin-based activity following complex formation. This minimal system supports the interpretation that disruption of actin organization at the AJ by clathrin depletion can be attributed directly to interference with events triggered by E-cadherin-mediated cell-cell adhesion.

An InlA-E-cadherin protein chimera allows cell adhesion to E-cadherin-expressing cells

We have previously demonstrated that the clathrin-actin interaction machinery is required for internalization of bacteria as well as E-cadherin-coated beads [5,14] and here we implicate the same molecular players in cell-cell adhesion. These observations suggest that cell-cell adhesion and internalization pathways involving E-cadherin trigger a common clathrin-mediated machinery. To address this hypothesis, we generated a model system that allows the study of the same ligand/receptor interaction in both cell adhesion and internalization. To this aim, we focused on the InlA/E-cadherin interaction, known to induce clathrin-mediated internalization of *Listeria monocytogenes*. We generated a chimeric InlA-E-cadherin protein in which the EC repeats involved in E-cadherin/E-cadherin interactions were replaced with the InlA LRR repeats that mediate InlA/E-cadherin interactions (Fig. 5a) [28]. To study the role of InlA/E-cadherin interactions in the context of cell-cell adhesion, the resulting InlA/E-cadherin chimera was expressed in HeLa cells, which do not express endogenous E-cadherin. We first verified the expression of the chimera by Western blot using an anti-InlA antibody (Fig. 5b) and then analyzed the localization of the chimera by immunofluorescence, using either an antibody against the intracellular domains of E-cadherin (Fig. S3a) or an anti-InlA antibody in non-permeabilized cells (Fig. S3b).

The functionality of the chimeric protein was then tested by incubating E-cadherin-coated beads with transfected HeLa cells (Fig. 5c). After 1 hour of incubation the chimera was efficiently recruited around the beads and, by differential labeling of beads before and after permeabilization, we observed that a large number of beads had been internalized (Fig. 5c). Clathrin was also recruited around internalized beads (Fig. S3c). Conversely, when chimera-transfected HeLa cells were incubated with *L. innocua* expressing InlA, we never observed bacterial adhesion or internalization (data not shown), in agreement with the established observation that InlA/InlA interactions do not occur [28].

HeLa cells expressing the chimeric InlA/E-cadherin protein were then co-cultured with Jeg3 cells expressing endogenous E-cadherin. After 24 h of co-culture, Jeg3 cells were labeled with an anti-E-cadherin antibody that targets the extracellular domain (absent in the InlA/E-cadherin chimera) and HeLa cells were labeled with an anti-InlA antibody (Fig. 5d). The InlA and E-cadherin labeling were strongly concentrated at the cell-cell contacts between

Jeg3 and transfected HeLa cells indicating that E-cadherin/InlA interaction had occurred (Fig. 5d). In some cases we observed the formation of vesicles positive for both E-cadherin and InlA, suggesting that endocytic events occurred during cell-cell adhesion (Fig. 5d, lower panels). Typical components of AJs such as α -catenin and actin were also concentrated at these hybrid junctions (Fig. S3d and e). The specificity of the InlA/E-cadherin interaction at cell-cell contacts was tested by co-culturing transfected HeLa cells with ELB1 cells expressing mouse E-cadherin. InlA interacts specifically with E-cadherin of human, gerbil, guinea pig and rabbit origin that share a proline at position 16. Mouse E-cadherin has a glutamate at position 16 and hence does not interact with InlA [29,30]. No accumulation of InlA or mouse E-cadherin was observed at cell-cell contacts between transfected HeLa cells and ELB1 cells (Fig. S3f) confirming the specificity of the adhesion sites we detected. These observations indicate that the molecular interactions between InlA and E-cadherin that mediate bacterial internalization can indeed support cell adhesion when InlA is expressed on the surface of adherent cells.

Cells expressing E-cadherin can internalize non-adherent cells expressing the InlA/E-cadherin chimera

On the basis of our observations that InlA/E-cadherin interactions occurring between two adherent epithelial cells result in cell-cell adhesion, we hypothesized that the interaction of bacterial surface proteins or ligand-coated beads with their respective cell receptors result in the internalization of bacteria and beads because they are not anchored in the surrounding environment. We therefore tested whether elimination of cell-matrix interactions would convert the InlA/E-cadherin interaction into an internalization signal, as in the case of bacterial infections. HeLa cells, transfected with the InlA/E-cadherin chimera, were detached from the substratum by trypsinization and then incubated with a confluent layer of Jeg3 cells. After 1 hour of incubation, cells were fixed and HeLa cells were differentially labeled with the anti-InlA antibody to distinguish internalized and extracellular cells (Fig. 6a). Jeg3 cells were labeled with the anti-E-cadherin antibody as described above. Remarkably, approximately 60% of detached transfected HeLa cells were internalized (Fig. 6b), or were in the process of being internalized by Jeg3 cells with evident concomitant recruitment of endogenous E-cadherin (as indicated by double labeling) (Fig. 6a). Non-transfected, as well as control-transfected HeLa cells, were never internalized by Jeg3 cells (Fig. 6b). In addition, transfected HeLa cells were never internalized by ELB1 cells expressing mouse E-cadherin (Fig. 6b).

HeLa cells transfected with E-cadherin carrying a GFP tag at its C-terminus, formed adherens junctions when incubated with Jeg3 cells expressing endogenous E-cadherin (Fig. S4a). However, when GFP-E-cadherin-expressing HeLa cells were trypsinized and incubated with adherent Jeg3 cells these latter efficiently internalized transfected HeLa cells (Fig. S4b). We used CLSEM to better visualize the internalization of transfected HeLa cells within Jeg3 cells. Transfected HeLa cells that contacted Jeg3 cells but were not yet internalized, exhibited a thin rim of E-cadherin labeling that was limited to the site of cell-cell contact (Fig. 7a top left panel and orthogonal views). HeLa cells that were fully internalized by Jeg3 cells were surrounded by a marked accumulation of E-cadherin fluorescence all along the cell Z-axis (Fig. 7b left panels). By SEM we observed recruitment of Jeg3 cell membranes that totally engulfed HeLa cells (Fig. 7b SEM). In some cases we could observe cell doublets where a transfected HeLa cell was in contact with a non-transfected HeLa cell. When the mixture of transfected and non-transfected HeLa cells interacted with Jeg3 cells, only the transfected HeLa cells were engulfed by Jeg3 cells (Fig. S4c).

We then followed the localization of clathrin in Jeg3 cells during cell-cell internalization and in all cases we observed strong recruitment of clathrin around HeLa cells transfected with

the InlA/E-cadherin chimera (Fig. 6c). Clathrin never accumulated near non-transfected or control-transfected HeLa cells (data not shown). Trypsinized, InlA/E-cadherin transfected HeLa cells were then incubated with Jeg3 cells depleted of CHC by siRNA and cell-cell internalization was quantified as described above. The efficiency of cell internalization was substantially reduced for Jeg3 cells depleted of CHC (Fig. 6b) and the majority of InlA/E-cadherin transfected HeLa cells were still detectable by extracellular staining. Importantly, E-cadherin recruitment around InlA/E-cadherin transfected HeLa cells was still evident in the absence of clathrin, confirming our previous observation that InlA/E-cadherin interactions, as well as E-cadherin/E-cadherin interactions are independent of clathrin at early stages of cell-cell or bacteria-cell interaction. Thus, our model system demonstrates that a cell adhesion pathway can be converted to an internalization pathway, depending on the mobility of one of the partners involved, which suggests, *Listeria* exploit this conversion for cellular invasion.

Discussion

Pathogens that adhere to host cells during infection often target proteins involved in cell adhesion such as integrins and E-cadherin [2-4]. In the case of pathogens that invade cells, these receptors are also hijacked for entry using a clathrin- and actin-dependent mechanism [6,7,14]. We recently reported that bacterial infections trigger the formation of clathrin-coated pits at bacterial/cell contact sites and that the formation of clathrin-coated pits precedes and is required for the rearrangements of actin needed for bacterial adhesion or uptake [14]. Here we show that the process of cell-cell adhesion triggers the same sequence of intracellular events that occur during bacterial infections. These include tyrosine-phosphorylation of CHC, as well as recruitment of the clathrin adaptor Dab2, the actin-binding protein Hip1R and the motor protein Myosin VI. In addition, we used siRNA to deplete cells of endogenous CHC and we show that clathrin recruitment at cell-cell contacts is required for subsequent reorganization of actin during the maturation of AJs. Because E-cadherin-coated beads bound to cells also recruit clathrin and actin and their uptake depends on these proteins, we propose that the actin alterations at the AJ following clathrin depletion result from direct interference with pathways triggered by transcellular E-cadherin complexes. We therefore suggest a novel role for clathrin as an actin organizer during the initiation of AJ formation that is independent of endocytosis and therefore distinct from clathrin-mediated E-cadherin internalization that occurs during AJ disruption [31,32].

To further explore the parallel between events triggered by E-cadherin/E-cadherin-mediated cell adhesion and those occurring during InlA/E-cadherin-mediated bacterial internalization, we developed a model system by generating a chimeric protein that contains the E-cadherin-binding domain of the *Listeria* protein InlA fused with the transmembrane and intracellular domains of E-cadherin. When HeLa cells that lack endogenous E-cadherin were transfected with this chimeric protein they were able to use the LRR domain of InlA to form hybrid AJs with Jeg3 expressing endogenous E-cadherin. The occasional observation of vesicles positive for both E-cadherin and InlA suggested the possibility that cell adhesion is accompanied by balanced “trogocytosis” [34], in which portions of one cell are internalized by the neighboring cell when both cells are anchored. We further observed that trypsinized (unanchored) HeLa cells expressing either InlA/E-cadherin or E-cadherin interact with and are internalized by adherent epithelial cells in a process reminiscent of bacterial uptake. This model system suggests that, in principle, the relative mobility of interacting partners may dictate the commitment to adhesion or internalization. We are aware that this is an artificial system demonstrating how bacteria could exploit adhesion for invasion, and cannot conclude that any such cell-cell internalization events based on E-cadherin interactions between epithelial cells occur in vivo. However, we note that a similar phenomenon of cell-cell internalization has been reported for other cell types. Macrophages can phagocytose

other cells [35] and cells from metastatic tumors internalize immune effector cells in a process called cell-cannibalism as a way to escape the immune response and acquire nutrients [36,37]. Interestingly, this phagocytic activity correlates with increased tumor expression of the human homologue of the protein phg1A from *Dictyostelium discoideum*[38] which uses AP1 and clathrin for phagocytosis [39]. In a related process called “entosis” mammary epithelial cells that have detached from the extracellular matrix, but have escaped programmed cell death, are internalized by neighbouring cells in suspension. This process differs from cannibalism in that the fate of the internalized cells may vary from degradation to intracellular duplication [40]. Of note, entosis is initiated, and dependent on, the establishment of E-cadherin dependent cell-cell adhesion. Here, with the goal of demonstrating that adhesion can be subverted for internalization, we developed a model system that reproduces a similar cell-in-cell phenomenon for non-metastatic epithelial cells. Further experiments will be required in order to assess whether this is a natural phenomenon of epithelial cells. We further note that in our model of conversion from adhesion to internalization, clathrin is involved in cell-cell internalization, whereas it has been previously shown that transcytosis of lymphocytes across epithelial cells is caveolin- and actin-dependent [41].

The E-cadherin-clathrin-actin dependent cell-in-cell internalization described here has parallels with the internalization of *Listeria*. Both pathways share properties of AJ formation. *Listeria* infection apparently represents bacterial exploitation of the junction formation pathway and its ability to convert to an internalization pathway. Through this analysis, we have now revealed a novel role for clathrin in organizing actin during cell-cell AJ formation, reinforcing the view that defining pathogen infection strategies can reveal unappreciated features of normal host cell pathways.

Materials and Methods

Cell lines

Jeg3 cells (human epithelial placental cells ATCC n°: HTB-36) HeLa cells (human cervix epithelial cells ATCC n°: CCL-2) and MDCK cells (Madin Darby Canine Kidney cells ATCC n°: CCL-34) were all grown in MEM medium containing Glutamax, non essential amino acids, sodium pyruvate and 10% Foetal Bovine Serum (FBS, Biowest, France).

Plasmids and siRNA sequences

Double-stranded RNA targeting CHC sequence 1: 5′-GGG AAU UCU UCG UAC UCC ATT-3′, sequence 2: 5′-GAU UAU CAA UUA CCG UAC ATT-3′, or CLC sequences (combined 5′-AAA GAC AGT TAT GCA GCT ATT-3′ against CLCa with 5′-AAG GAA CCA GCG CCA GAG TGA-3′ against CLCb), Cy3-tagged CHC-targeted double stranded RNA: 5′-Cy3/GGG CAA UUC AAA GAU AUC ATT-3′ and control siRNA sequences were obtained from Ambion. Double-stranded RNA targeting the Hip1R sequence 1: 5′-AAC AGG AAC UUG CCA CAA GCC-3′, sequence 2: 5′-ACC GGA GAA TCT CAT TGA GAT CTT-3′ and control siRNA sequences were obtained from Qiagen. Double-stranded RNA targeting the Myosin VI sequence 1: 5′-GCU GGC AGU UCA UAG GAA UTT-3′, sequence 2: 5′-AUU CCU AUG AAC UGC CAG CTT-3′ and control siRNA sequences were obtained from Eurogentec. Double-stranded RNA targeting the Dab2 sequence 1: 5′-GCA AAG AUA UCC UGU UAG UTT-3′, sequence 2: 5′-GAA CCA GCC UUC ACC CUU UTT-3′ and control siRNA sequences were obtained from Thermo Scientific. GFP-tagged E-cadherin was kindly provided by Prof. W.J. Nelson (Stanford University, CA); GFP-tagged clathrin light chain was kindly provided by Prof. Tomas Kirchhausen (Harvard Medical School, MA). The In1A/E-cadherin chimera was generated as follows: the region of In1A encompassing the LRR repeats and the inter repeat region (IR)

was PCR amplified from *L. monocytogenes* colonies (BUG600) using InlA-Ecad Fw (5' CTG CTG CAG GTC TCC TCT TGG CTC TGC CAG GAG GCT ACA ATT ACA CAA GAT ACT CCT AT 3') and InlA-Ecad Rev (5' GAC GCC GGC AGG ATT TTT CGT AAA TTG AGC GTA CAG 3') that allowed the integration of a PstI and NgoMIV digestion sites that were used for digestion. We then digested a pcDNA3-E-cadherin vector with NgoMIV producing two fragments, one containing the transmembrane and intracellular domains of E-cadherin and the other one the signal peptide and the EC repeats. The latter fragment was digested again with PstI generating a fragment containing only the EC repeats of E-cadherin and the other one containing the E-cadherin signal peptide. We then discarded the fragment containing the EC repeats and fused the other two fragments of E-cadherin with the InlA PCR product. We thus generated a chimera that maintained the signal peptide, the transmembrane and the intracellular domains of E-cadherin and substituted the EC-repeats region with the LRR and IR regions of InlA.

Antibodies and reagents

HECD1 anti-human E-cadherin (extracellular region) and ECCD-2 anti-mouse E-cadherin antibodies were obtained from Takara (Shiga, Japan); 24E10 anti-human E-cadherin antibody (intracellular region) was from Cell Signaling Technology; anti-Hip1R and anti p34 polyclonal antibodies were from Millipore (CA, USA); anti- α -catenin polyclonal antibody, anti-Dab2 polyclonal antibody, anti-Myosin VI polyclonal antibody were from Santa Cruz Biotechnology (Santa Cruz, CA); anti-GAPDH monoclonal antibody was from Abcam (Cambridge, UK); anti mDia1 monoclonal antibody was from BD Transduction Laboratories; X22 anti-CHC monoclonal antibody, anti-CLC polyclonal antibody and anti phospho-CHC were produced in our laboratory as previously described [14,27,42], anti-InlA polyclonal antibody R302 and anti-InlA monoclonal antibody L7.7 were produced in our laboratory. Alexa Fluor 647-conjugated, Cy3-conjugated and FITC-conjugated Phalloidin and Hoechst were from Molecular Probes (Leiden, The Netherlands). Paraformaldehyde was obtained from Electron Microscopy Solutions (EMS, Hatfield, PA).

Immunofluorescence analysis

Cells were fixed in 4% paraformaldehyde in PBS at room temperature, rinsed in PBS and incubated in blocking solution (0.5% BSA, 50 mM NH₄Cl in PBS, pH 7.4). 0.05% saponin was added to the blocking solution where needed. Cells were then incubated with the primary antibodies diluted in blocking solution for 1 hour at room temperature, rinsed 5 times in PBS and further incubated for 45 minutes with the secondary antibodies diluted in the blocking solution. Where needed, fluorescent phalloidin was added to the secondary antibodies to label actin. Where indicated, cells were subjected to cytosolic extraction before fixation. Briefly, cells were incubated 30 seconds in extraction buffer (80mM PIPES pH6.9, 0.9mM EGTA, 0.9mM EDTA, 30% glycerol) containing 0.1% Triton X-100, washed in extraction buffer and fixed in 3% paraformaldehyde in extraction buffer. After labeling, coverslips were mounted using Fluoromount medium (EMS, PA). Where needed, Hoechst was added to the mounting medium for nuclei visualization. Samples were analyzed with a Zeiss Axiovert 135 epifluorescence microscope (Carl Zeiss) connected to a CCD camera. Images were acquired alternatively with a 100 \times , 63 \times or 40 \times oil immersion objectives and processed with MetaMorph (Universal Imaging Corp.). ImageJ software was used for image analysis and quantifications. Differential immunofluorescence labeling for extracellular and total beads and cells was performed as previously described for bacterial infections [5].

Coated-bead internalization assays

E-cadherin-coated bead internalization was performed as previously described [5].

Transient transfections

For DNA transient transfection cells were plated to 80% confluency and transfected using Gene Juice (Merck) according to manufacturers' instructions. Cells were incubated 24 hours with the transfectant before the experiment. For siRNA transfection 2×10^5 /ml cells were mixed with siRNA and Lipofectamine RNAiMAX prior to plating according to manufacturers' instructions for reverse transfections. Cells were probed for siRNA efficacy 72h after transfection by Western blot.

Calcium-jump assay

MDCK were cultured in glass-bottomed Petri dishes and transfected with GFP-tagged CLC as described above. Cells were then incubated until they reached confluency (48 h approximately), rinsed 3 times in PBS and incubated in HBSS culture medium without calcium. Cells were then imaged with a $40\times$ oil immersion objective using an epifluorescence microscope equipped with a temperature- and CO₂-controlled chamber. Images were acquired every 2 minutes and as cells separated in response to calcium removal, complete culture medium was re-added to cells and imaging was continued for approximately 15 hours. Cells were then fixed after imaging and processed for indirect immunofluorescence where actin was labeled with fluorescent phalloidin and E-cadherin with the HECD1 antibody.

Cell-cell adhesion assay and Correlative Light Scanning Electron Microscopy (CLSEM)

To follow the effects of clathrin depletion during the onset of cell-cell adhesion, Jeg3 cells were transfected with Cy3-tagged control or clathrin heavy chain-targeted siRNA sequences as described above. Cells were trypsinized 48 h after transfection and re-seeded onto glass coverslips overnight before the experiment to allow the formation of new cell-cell contacts. Cells were then fixed and processed for immunofluorescence where actin and E-cadherin at cell-cell contacts were labeled by Cy5-tagged phalloidin and anti-E-cadherin HECD1 antibody respectively. The frequency of E-cadherin and actin recruitment at cell-cell contact was quantified by fluorescence microscopy where approximately 100 cells were analyzed for each condition. The fluorescence profile of E-cadherin and actin across cell-cell contact was measured along arbitrary lines perpendicular to cell junctions. Fluorescence measurements were applied to an average of 50 cells and multiple cell-cell junctions were probed for each cell. For CLSEM microscopy, cells were trypsinized the day before the experiment and re-seeded onto glass-bottomed Petri dishes with a Cellocator grid engraved for cell localization (MatTek Corporation). On the day of the experiment cells were permeabilized before fixation in a cytoskeleton-stabilizing buffer (1% triton, 4% PEG 8000, 10mM PIPES, 0.1mM EGTA, 0.1mM MgCl₂) at 37° C. Cells were rinsed and fixed in 3% paraformaldehyde and 0.05% glutaraldehyde. Cells were then labeled with fluorescent phalloidin as previously described and imaged with an epifluorescence microscope. In parallel, a sample of siRNA-transfected cells was used to test the efficacy of clathrin knock down by Western blot. Alternatively, Jeg3 cells were cultured onto glass-bottomed petri dishes with a Cellocator grid engraved and subjected to the cell internalization assay (see below). In all cases, for subsequent scanning electron microscopy analysis, the position of the cells of interest were identified on the Cellocator grid and cells were fixed in 2.5% glutaraldehyde in 0.2M cacodylate buffer (pH7.2) overnight at 4°C, then washed for 5 minutes three times in 0.2M cacodylate buffer (pH7.2), postfixed for 1 hour in 1% osmium, and rinsed with distilled water. Cells were dehydrated through a graded ethanol series followed by critical point drying with CO₂. Dried specimens were sputter-coated twice with gold/palladium with a gun ionic evaporator PEC 682. The coordinates of the correlative imaged with fluorescent microscopy were recovered in a JEOL JSM 6700F field emission scanning electron microscope operating at 7 kV. The same cells were then observed and imaged by using the secondary electron image detector.

Hybrid junctions and cell internalization assays

HeLa cells and Jeg3 cells were cultured separately into 6-wells plates and HeLa cells were transfected with the InlA/E-cadherin chimera as previously described. 24 h after transfection HeLa and Jeg3 cells were trypsinized and co-cultured onto glass coverslips in 24-wells plates. Cells were then spinned 2 min at 1000 rpm to synchronize cell adhesion to the substrate and incubated overnight at 37° C. Cells were then fixed in 4% paraformaldehyde and processed for immunofluorescence where transfected HeLa cells were labeled by the anti InlA antibody and Jeg3 cells by the anti-E-cadherin antibody HECD1. For cell-cell internalization, HeLa cells were cultured and transfected as above and Jeg3 cells were cultured directly onto glass coverslips in 24-wells plates. 24 h after transfection HeLa cells were trypsinized and incubated on a confluent layer of Jeg3 cells. Cells were spinned as described above and incubated 1 h at 37° C. Cells were then fixed as above and differentially labeled for InlA before and after permeabilization to distinguish extracellular and intracellular cells. Jeg3 cells were labeled with the anti-E-cadherin antibody HECD1. Cell-cell internalization was quantified by immunofluorescence where approximately 100 transfected HeLa cells were counted for each condition.

Supplementary Material

Refer to Web version on PubMed Central for supplementary material.

Acknowledgments

This work was supported by Institut Pasteur, Inserm, INRA, ERC (Advanced Grant 233348) to P.C. and NIH grant GM038093 to F.M.B. M.B. was supported by the Pasteur Roux Fellowship. A.T.-A. was an EMBO long-term fellow. A.K. is a recipient of a scholarship from the Pasteur-Paris University International Doctoral Program/ Institut Carnot Maladies Infectieuses. P.C. is an international research scholar of the Howard Hughes Medical Institute. The authors have no conflict of interest.

References

1. Cavallaro U, Christofori G. Cell adhesion and signalling by cadherins and Ig-CAMs in cancer. *Nat Rev Cancer*. 2004; 4:118–132. [PubMed: 14964308]
2. Bonazzi M, Cossart P. Impenetrable barriers or entry portals? The role of cell-cell adhesion during infection. *JCB*. 2011; 195:349–358. [PubMed: 22042617]
3. Knodler LA, Celli J, Finlay BB. Pathogenic trickery: deception of host cell processes. *Nat Rev Mol Cell Biol*. 2001; 2:578–588. [PubMed: 11483991]
4. Pizarro-Cerdá J, Cossart P. Bacterial adhesion and entry into host cells. *Cell*. 2006; 124:715–727. [PubMed: 16497583]
5. Bonazzi M, Veiga E, Pizarro-Cerdá J, Cossart P. Successive post-translational modifications of E-cadherin are required for InlA-mediated internalization of *Listeria monocytogenes*. *Cell Microbiol*. 2008; 10:2208–2222. [PubMed: 18624796]
6. Veiga E, Cossart P. *Listeria* hijacks the clathrin-dependent endocytic machinery to invade mammalian cells. *Nat Cell Biol*. 2005; 7:894–900. [PubMed: 16113677]
7. Veiga E, Guttman JA, Bonazzi M, Boucrot E, Toledo-Arana A, Lin AE, Enninga J, Pizarro-Cerdá J, Finlay BB, Kirchhausen T, Cossart P. Invasive and adherent bacterial pathogens co-opt host clathrin for infection. *Cell Host Microbe*. 2007; 2:340–351. [PubMed: 18005755]
8. Patel SD, Chen CP, Bahna F, Honig B, Shapiro L. Cadherin-mediated cell-cell adhesion: sticking together as a family. *Current Opinion in Structural Biology*. 2003; 13:690–698. [PubMed: 14675546]
9. Roy F, Berx G. The cell-cell adhesion molecule E-cadherin. *Cell Mol Life Sci*. 2008; 33
10. Drees F. α -catenin is a molecular switch that binds E-cadherin- β -catenin and regulates actin-filament assembly. *Cell*. 2005; 123:903–915. [PubMed: 16325583]

11. Verma S, Shewan AM, Scott JA, Helwani FM, Elzen den NR, Miki H, Takenawa T, Yap AS. Arp2/3 activity is necessary for efficient formation of E-cadherin adhesive contacts. *J Biol Chem.* 2004; 279:34062–34070. [PubMed: 15159390]
12. Yamada S, Pokutta S, Drees F, Weis WI, Nelson WJ. Deconstructing the cadherin-catenin-actin complex. *Cell.* 2005; 123:889–901. [PubMed: 16325582]
13. Sousa S, Cabanes D, Bougnères L, Lecuit M, Sansonetti P, Tran-Van-Nhieu G, Cossart P. Src, cortactin and Arp2/3 complex are required for E-cadherin-mediated internalization of *Listeria* into cells. *Cell Microbiol.* 2007; 9:2629–2643. [PubMed: 17627624]
14. Bonazzi M, Vasudevan L, Mallet A, Sachse M, Sartori A, Prévost M-C, Roberts A, Taner S, Wilbur J, Brodsky F, Cossart P. Clathrin phosphorylation is required for actin recruitment at sites of bacterial adhesion and internalization. *JCB.* 2011; 195:525–536. [PubMed: 22042622]
15. Crotzer VL, Mabardy AS, Weiss A, Brodsky FM. T cell receptor engagement leads to phosphorylation of clathrin heavy chain during receptor internalization. *J Exp Med.* 2004; 199:981–991. [PubMed: 15067034]
16. Stoddart A, Dykstra ML, Brown BK, Song W, Pierce SK, Brodsky FM. Lipid rafts unite signaling cascades with clathrin to regulate BCR internalization. *Immunity.* 2002; 17:451–462. [PubMed: 12387739]
17. Wilde A, Beattie EC, Lem L, Riethof DA, Liu SH, Mobley WC, Soriano P, Brodsky FM. EGF receptor signaling stimulates SRC kinase phosphorylation of clathrin, influencing clathrin redistribution and EGF uptake. *Cell.* 1999; 96:677–687. [PubMed: 10089883]
18. Carreno S, Engqvist-Goldstein AE, Zhang CX, McDonald KL, Drubin DG. Actin dynamics coupled to clathrin-coated vesicle formation at the trans-Golgi network. *J Cell Biol.* 2004; 165:781–788. [PubMed: 15210728]
19. Chen C-Y, Brodsky FM. Huntingtin-interacting protein 1 (Hip1) and Hip1-related protein (Hip1R) bind the conserved sequence of clathrin light chains and thereby influence clathrin assembly in vitro and actin distribution in vivo. *J Biol Chem.* 2005; 280:6109–6117. [PubMed: 15533940]
20. Engqvist-Goldstein AEY. The actin-binding protein Hip1R associates with clathrin during early stages of endocytosis and promotes clathrin assembly in vitro. *J Cell Biol.* 2001; 154:1209–1224. [PubMed: 11564758]
21. Engqvist-Goldstein AEY, Zhang CX, Carreno S, Barroso C, Heuser JE, Drubin DG. RNAi-mediated Hip1R silencing results in stable association between the endocytic machinery and the actin assembly machinery. *Mol Biol Cell.* 2004; 15:1666–1679. [PubMed: 14742709]
22. Le Clairche C, Pauly BS, Zhang CX, Engqvist-Goldstein AEY, Cunningham K, Drubin DG. A Hip1R-cortactin complex negatively regulates actin assembly associated with endocytosis. *EMBO J.* 2007; 26:1199–1210. [PubMed: 17318189]
23. Newpher TM, Idrissi FZ, Geli MI, Lemmon SK. Novel function of clathrin light chain in promoting endocytic vesicle formation. *Mol Biol Cell.* 2006; 17:4343–4352. [PubMed: 16870700]
24. Wilbur JD, Chen CY, Manalo V, Hwang PK, Fletterick RJ, Brodsky FM. Actin Binding by Hip1 (Huntingtin-interacting Protein 1) and Hip1R (Hip1-related Protein) Is Regulated by Clathrin Light Chain. *Journal of Biological Chemistry.* 2008; 283:32870–32879. [PubMed: 18790740]
25. McLachlan RW, Kraemer A, Helwani FM, Kovacs EM, Yap AS. E-cadherin adhesion activates c-Src signaling at cell-cell contacts. *Mol Biol Cell.* 2007; 18:3214–3223. [PubMed: 17553930]
26. Pang JH, Kraemer A, Stehens SJ, Frame MC, Yap AS. Recruitment of phosphoinositide 3-kinase defines a positive contribution of tyrosine kinase signaling to E-cadherin function. *J Biol Chem.* 2005; 280:3043–3050. [PubMed: 15556934]
27. Brodsky FM. Clathrin structure characterized with monoclonal antibodies. I. Analysis of multiple antigenic sites. *J Cell Biol.* 1985; 101:2047–2054. [PubMed: 2415533]
28. Schubert WD, Urbanke C, Ziehm T, Beier V, Machner MP, Domann E, Wehland J, Chakraborty T, Heinz DW. Structure of internalin, a major invasion protein of *Listeria monocytogenes*, in complex with its human receptor E-cadherin. *Cell.* 2002; 111:825–836. [PubMed: 12526809]
29. Bonazzi M, Lecuit M, Cossart P. *Listeria monocytogenes* internalin and E-cadherin: from structure to pathogenesis. *Cell Microbiol.* 2009

30. Lecuit M, Dramsi S, Gottardi C, Fedor-Chaiken M, Gumbiner B, Cossart P. A single amino acid in E-cadherin responsible for host specificity towards the human pathogen *Listeria monocytogenes*. *EMBO J*. 1999; 18:3956–3963. [PubMed: 10406800]
31. Le TL, Joseph SR, Yap AS, Stow JL. Protein kinase C regulates endocytosis and recycling of E-cadherin. *Am J Physiol, Cell Physiol*. 2002; 283:C489–99. [PubMed: 12107059]
32. de Beco S, Gueudry C, Amblard F, Coscoy S. Endocytosis is required for E-cadherin redistribution at mature adherens junctions. *Proc Natl Acad Sci USA*. 2009
33. Delva E, Kowalczyk AP. Regulation of Cadherin Trafficking. *Traffic*. 2009; 10:259–267. [PubMed: 19055694]
34. Ahmed KA, Munegowda MA, Xie Y, Xiang J. Intercellular trogocytosis plays an important role in modulation of immune responses. *Cell Mol Immunol*. 2008; 5:261–269. [PubMed: 18761813]
35. Tsai RK, Discher DE. Inhibition of “self” engulfment through deactivation of myosin-II at the phagocytic synapse between human cells. *J Cell Biol*. 2008; 180:989–1003. [PubMed: 18332220]
36. Lugini L, Matarrese P, Tinari A, Lozupone F, Federici C, Iessi E, Gentile M, Luciani F, Parmiani G, Rivoltini L, Malorni W, Fais S. Cannibalism of live lymphocytes by human metastatic but not primary melanoma cells. *Cancer Res*. 2006; 66:3629–3638. [PubMed: 16585188]
37. Wang S, Guo Z, Xia P, Liu T, Wang J, Li S, Sun L, Lu J, Wen Q, Zhou M, Ma L, Ding X, Wang X, Yao X. Internalization of NK cells into tumor cells requires ezrin and leads to programmed cell-in-cell death. *Cell Res*. 2009; 19:1350–1362. [PubMed: 19786985]
38. Lozupone F, Perdicchio M, Brambilla D, Borghi M, Meschini S, Barca S, Marino ML, Logozzi M, Federici C, Iessi E, de Milito A, Fais S. The human homologue of *Dictyostelium discoideum* phg1A is expressed by human metastatic melanoma cells. *EMBO Rep*. 2009; 10:1348–1354. [PubMed: 19893578]
39. Lefkir Y, Malbouyres M, Gotthardt D, Ozinsky A, Cornillon S, Bruckert F, Aderem AA, Soldati T, Cosson P, Letourneur F. Involvement of the AP-1 adaptor complex in early steps of phagocytosis and macropinocytosis. *Mol Biol Cell*. 2004; 15:861–869. [PubMed: 14617812]
40. Overholtzer M, Mailleux A, Mouneimne G, Normand G, Schnitt S, King R, Cibas E, Brugge J. A nonapoptotic cell death process, entosis, that occurs by cell-in-cell invasion. *Cell*. 2007; 131:966–979. [PubMed: 18045538]
41. Millán J, Hewlett L, Glyn M, Toomre D, Clark P, Ridley AJ. Lymphocyte transcellular migration occurs through recruitment of endothelial ICAM-1 to caveola- and F-actin-rich domains. *Nat Cell Biol*. 2006; 8:113–123. [PubMed: 16429128]
42. Acton S, Wong D, Parham P, Brodsky F, Jackson A. Alteration of clathrin light chain expression by transfection and gene disruption. *Mol Biol Cell*. 1993; 4:647. [PubMed: 8374173]
43. Esk C, Chen CY, Johannes L, Brodsky FM. The clathrin heavy chain isoform CHC22 functions in a novel endosomal sorting step. *J Cell Biol*. 2010; 188:131. [PubMed: 20065094]

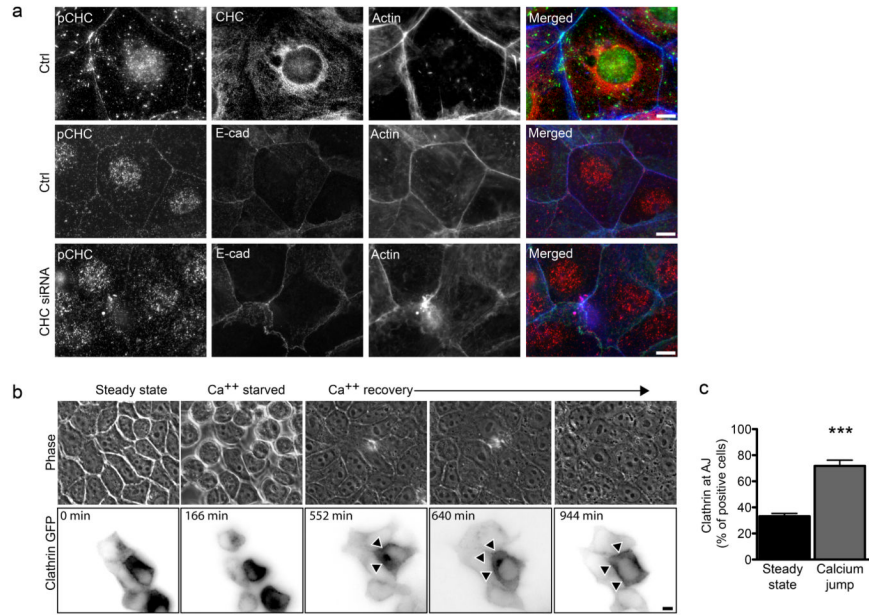


Figure 1. AJ formation induces CHC phosphorylation and the recruitment of clathrin at cell-cell contacts a. Jeg3 cells were left untreated (top), incubated with non-targeting (middle) or CHC-targeting (bottom) siRNA sequences, seeded and allowed to form AJs for 12 to 16 hours. Cells were then fixed and labeled for immunofluorescence as indicated. b. Representative images (acquired live) of MDCK cells transfected with CLC-GFP and subjected to the calcium jump assay to follow clathrin recruitment at cell-cell contacts (arrowheads) during the formation of adherens junctions. c. MDCK cells at steady state or 12h after the calcium jump were fixed and labeled for clathrin, E-cadherin and actin. The frequency of clathrin recruitment at cell-cell junctions was assayed by fluorescence microscopy. In c values are means (\pm standard deviation) of three independent experiments. Asterisks represent p values (***) = $p < 0.001$, Student t-test). Scale bars 10 μ m.

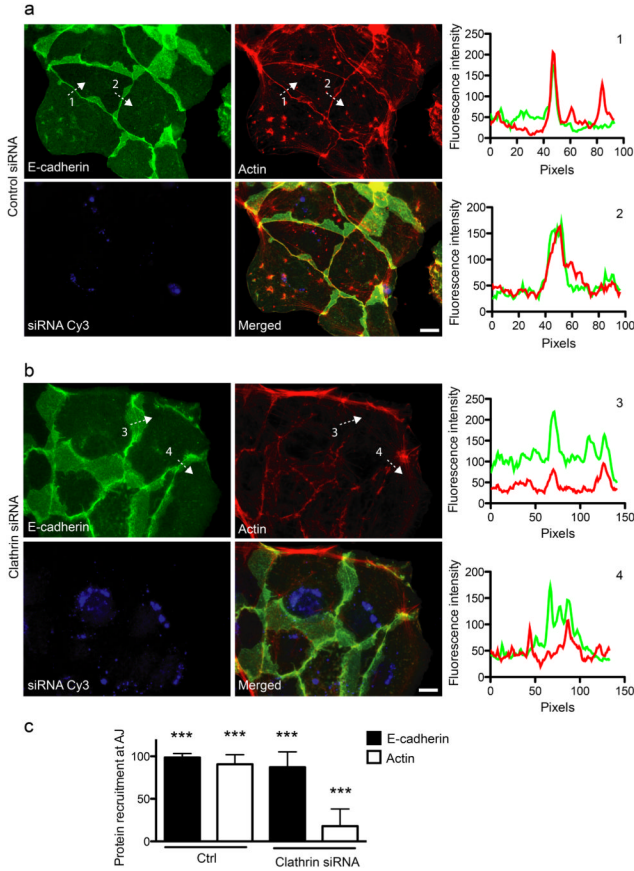


Figure 2. Clathrin is required for actin recruitment at cell-cell contacts. Jeg3 cells were transfected with Cy3-tagged control (a) or clathrin-targeted siRNAs (b). 48h after transfection cells were trypsinized and seeded on glass coverslips to allow the formation of new adherens junctions. 12 h after seeding, cells were fixed and labeled for E-cadherin (green) and actin (red). The fluorescence intensity profiles along arbitrary lines drawn perpendicular to cell-cell contacts (dashed arrows 1, 2, 3 and 4) was measured for E-cadherin (green) and actin (red) (Right charts, numbers correspond to the dashed profiles on the left panels). c. Quantification of control and clathrin knocked-down cells presenting E-cadherin and actin at cell-cell junctions. Values are means (\pm standard deviation) of three independent experiments where approximately 100 cells were analyzed for each condition. Asterisks represent p values (***) = $p < 0.001$, Student t-test). Scale bars 10 μ m.

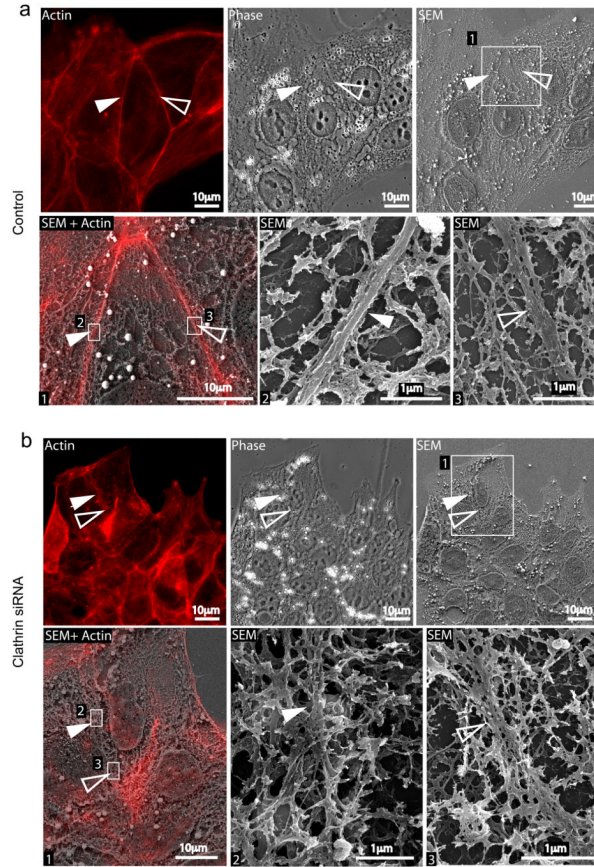


Figure 3. CLSEM analysis of actin at cell-cell contacts in control and clathrin depleted cells. Jeg3 cells transfected with Cy3-tagged control (a) or anti-clathrin siRNAs (b) were permeabilized and labeled for actin (red). Cells were first imaged with an epifluorescence microscope (Actin and phase panels in a and b) and then processed for scanning electron microscopy (SEM). The ultrastructure of the cytoskeleton in control and clathrin knocked down cells was compared. In both a and b, panels 2 and 3 represent higher magnifications of the boxed areas in panel 1. Full and empty arrowheads point at actin structures at cell-cell contacts.

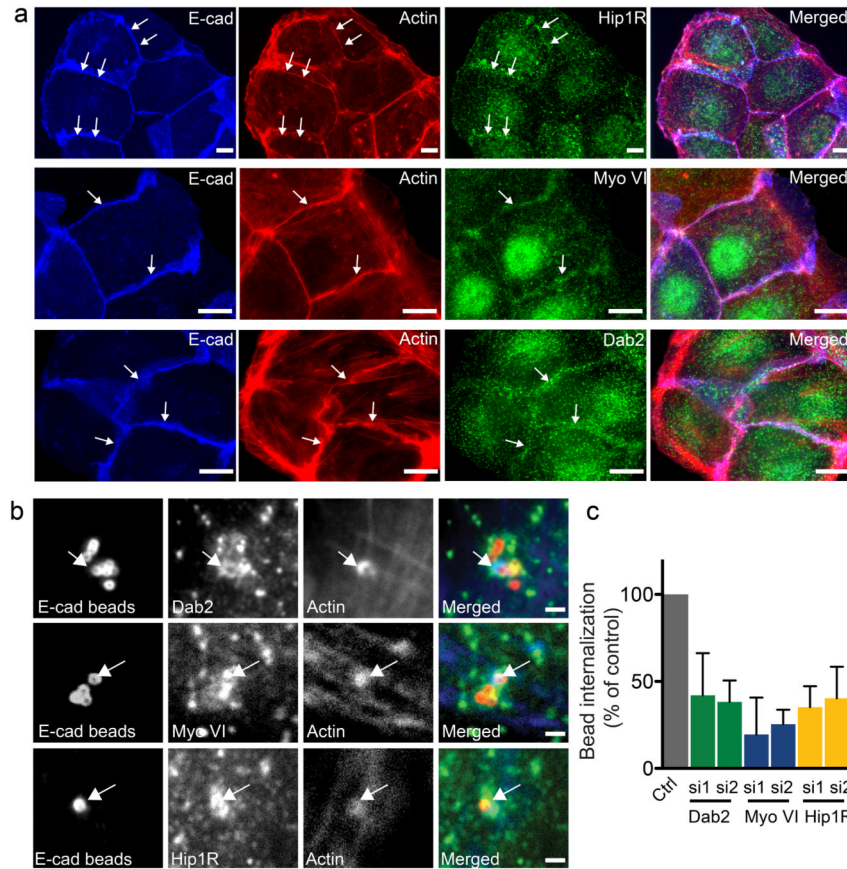


Figure 4. The clathrin/actin interaction machinery is recruited at sites of adherens junctions formation. a. JEG3 cells were seeded and allowed to form AJs for 12 hours. Cells were then fixed and labeled for E-cadherin (blue), actin (red) and Hip1R, Myosin VI, Dab2 (green). Arrows indicate sites where Hip1R Myosin VI and Dab2 accumulate with E-cadherin and actin at adherens junctions. Scale bars 10 μm . b JEG3 cells were incubated with E-cadherin-coated latex beads for 15 min, fixed and processed for immunofluorescence. Arrows point at sites of colocalization. c. JEG3 cells were transfected with two siRNA sequences targeted to either Dab2, Myosin VI or Hip1R or with scrambled control siRNA sequences and incubated 1 h with E-cadherin-coated latex beads. Cells were then fixed and differentially labeled to discriminate intracellular and extracellular beads and the efficiency of beads internalization was quantified by fluorescence microscopy. Values are means (\pm standard deviation) of three independent experiments where approximately 100 beads were counted for each condition. Asterisks represent p values. Scale 10 μm (d).

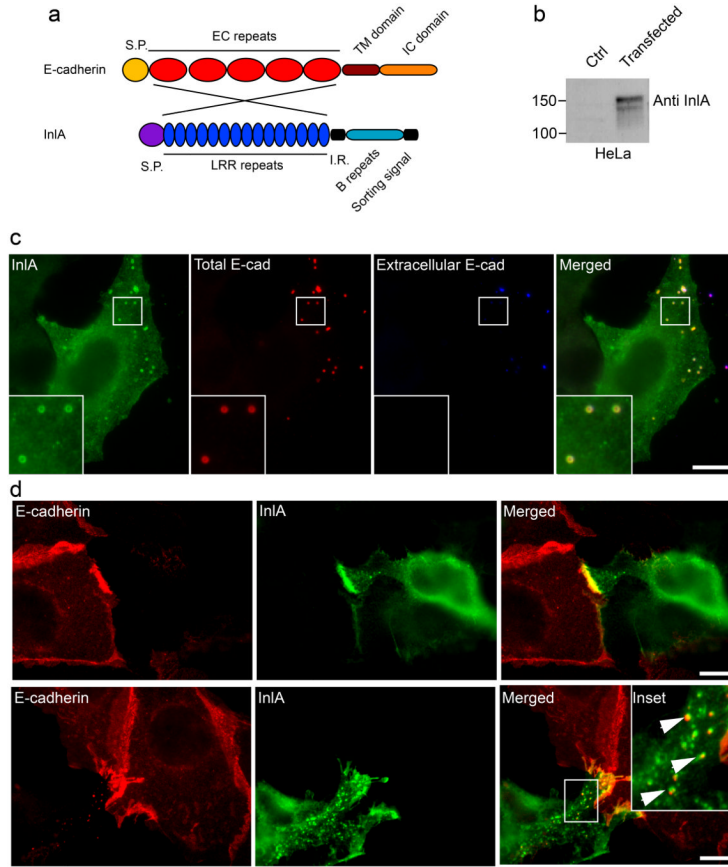


Figure 5. InlA/E-cadherin interactions generate hybrid cell-cell junctions. a. The InlA/E-cadherin chimeric protein was generated by substituting the EC repeats of E-cadherin with the LRR repeats of the *Listeria monocytogenes* surface protein InlA. b. HeLa cells were transfected with a control plasmid or with a plasmid containing the chimeric DNA and the expression of the chimera was tested by Western blots with an InlA-specific antibody. c. HeLa cells transfected with the InlA-E-cadherin chimera were incubated with E-cadherin-coated beads for 1 h. Beads were labeled with an anti-E-cadherin antibody before (blue) and after permeabilization (red) to distinguish extracellular and intracellular beads and cells were labeled with an anti-InlA antibody (green) to detect transfected cells. d. HeLa cells transfected with the InlA/E-cadherin chimera were co-cultured with Jeg3 cells expressing endogenous E-cadherin. After an overnight incubation cells were fixed and labeled with an antibody against the extracellular domain of E-cadherin, that specifically recognizes endogenous E-cadherin (red), and with an InlA-specific antibody (green). When cell-cell contacts were more interdigitated we could observe the presence of endocytic vesicles positive for both InlA (green) and E-cadherin (red). Scale bars 10 μ m.

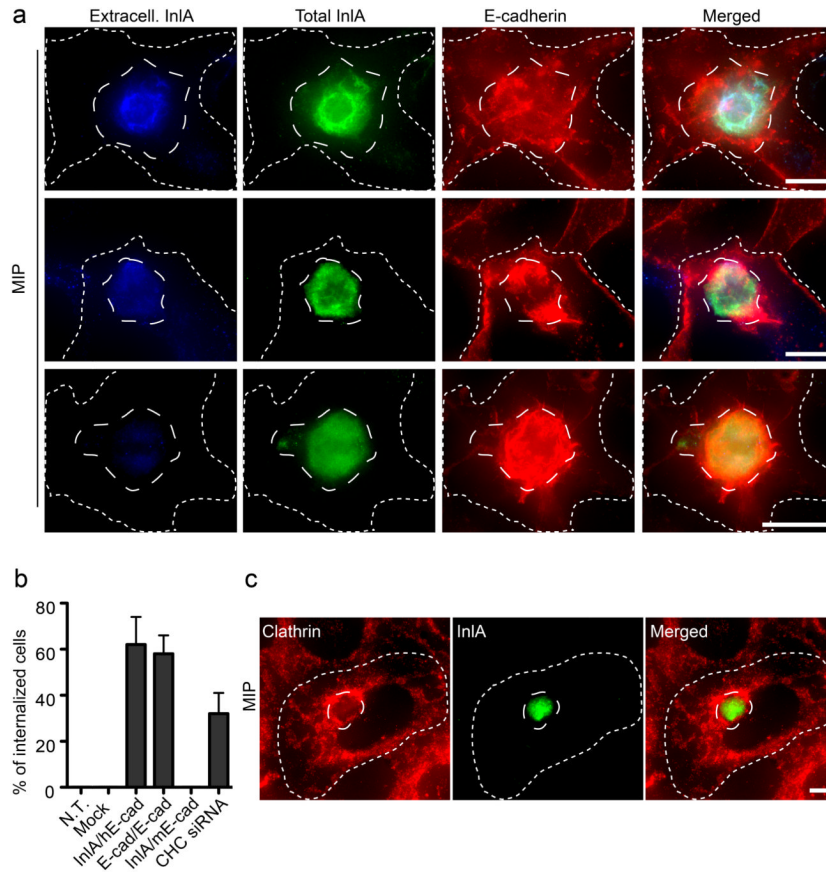


Figure 6. Cell adhesion mediates cell-in-cell events. **a.** Maximum intensity projections (MIP) of image stacks acquired along the z-axis of HeLa cells transfected with the InlA/E-cadherin chimera (long-dashed outline), trypsinized and incubated for 1 h on a confluent layer of JEG3 cells (short-dashed outline). HeLa cells were labeled for InlA before permeabilization (blue) to detect extracellular cells and after permeabilization (green) to detect total HeLa cells. JEG3 cells were labeled for E-cadherin (red). Images represent different stages of cell-cell internalization. **b.** HeLa cells were either left untransfected (N.T.), transfected with an empty vector (mock), with the InlA/E-cadherin chimera (InlA/hE-cad) or with GFP-tagged E-cadherin (E-cad/E-cad). Cells were trypsinized and incubated for 1h on adherent JEG3 cells. As a control, HeLa cells transfected with the InlA/E-cadherin chimera were trypsinized and incubated for 1h on ELB1 cells expressing mouse E-cadherin (InlA/mEcad). To test the role of clathrin in cell-in-cell events HeLa cells transfected with the InlA/E-cadherin chimera were incubated for 1h with adherent JEG3 cells where clathrin heavy chain (CHC) had been previously knocked down by siRNA. In all cases the frequency of cell-in-cell events was quantified by fluorescence microscopy were HeLa cells were differentially labeled before and after permeabilization. Values are means (\pm standard deviation) of three independent experiments where approximately 100 cells were analyzed for each condition. **c.** Maximum intensity projections (MIP) of image stacks acquired along the z-axis of HeLa cells transfected with the InlA/E-cadherin chimera (long-dashed outline), trypsinized and incubated for 1 h on a confluent layer of JEG3 cells (short-dashed outline). Cells were labeled for InlA (green) and clathrin (red). Scale bars 10 μ m.

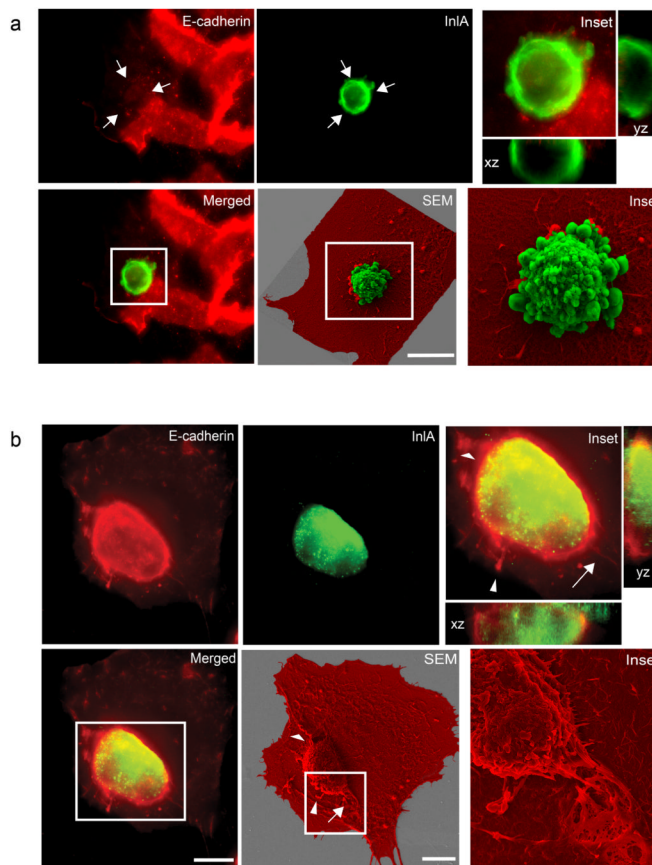


Figure 7. CLSEM analysis of cell-in-cell events Early (a) and late (b) stages of cell-in-cell events. HeLa cells transfected with the InlA/E-cadherin chimera were trypsinized and incubated for 1 h on a confluent layer of Jeg3 cells. HeLa cells were labeled for InlA (green) and Jeg3 cells were labeled for E-cadherin (red). Cells were imaged along the z-axis to visualize E-cadherin recruitment around transfected HeLa cells (xz and yz orthogonal views of insets). Using CLSEM the same cells were scanned at the electron microscope to better visualize cell-cell internalization (SEM and corresponding insets. Jeg3 cells are pseudo-colored in red, transfected HeLa cells are pseudo-colored in green). Arrows indicate examples of correlated structures visualized by immunofluorescence and scanning electron microscopy. Scale bars 10 μm .